Eur. Phys. J. Special Topics **227**, 45–54 (2018)

https://doi.org/10.1140/epjst/e2018-00112-y

THE EUROPEAN PHYSICAL JOURNAL SPECIAL TOPICS

Regular Article

Shockless spalling characterization of ceramics in a 1D-stress state

Benjamin Erzar[a]

CEA, DAM, CEA-Gramat, 46500 Gramat, France

Received 6 November 2017 / Received in final form 12 January 2018
Published online 10 September 2018

Abstract. Ceramics are particularly interesting as protective materials due to their high compressive strength. However the maximum tensile stress withstood by these materials is usually lower by one order of magnitude. To study the dynamic strength in tension, spalling tests are commonly performed. In this work, a new spalling configuration is presented to characterize brittle materials such as ceramics at ultra-high strain-rates of about 10^3–10^4 s^{-1} in a one-dimensional stress state. To do so, a specific test is designed in which the ceramic specimen is a bar with a 3 mm radius. This geometry is chosen to ensure a one-dimensional stress state in the cylindrical specimen avoiding wave dispersion during the propagation of the loading pulse. Finally, the first experimental validation tests conducted at the CEA-Gramat with the pulsed power generator called GEPI are reported.

1 Introduction

The performance of ceramic materials subjected to high loading rates is a primary concern to design efficient armors. Several techniques have been introduced in recent decades to characterize the dynamic strength of brittle materials. Shock characterization by means of plate impact experiments allows the spalling strength of a brittle sample to be determined, such as ceramics [1–4]. Other groups have performed indirect tensile experiments, such as Brazilian tests [5]. A review focused on experimental characterization of armor ceramics gathers a large amount of data obtained through these techniques [6]. Recently, the use of a pulsed power generator to produce ramp loading has been used to conduct spalling tests with a good knowledge of the strain-rate at failure [7,8]. These experiments have highlighted the rate-sensitivity of the dynamic tensile strength of ceramics in the range 10^3–10^4 s^{-1}.

In this work, a new methodology is proposed using the GEPI machine [9,10]. This high-pulsed power generator has already been used to characterize the spalling strength of an alumina ceramic [7,8], silicon carbides [11] and a mortar [12]. The particularity of the new configuration consists in conducting a spalling test in a one-dimensional stress state. To do so, a cylindrical ceramic specimen was designed to limit the dispersive effects during the loading pulse propagation. First, the main equations describing the propagation of elastic waves in rods are introduced. Then, finite

[a] e-mail: benjamin.erzar@cea.fr

element simulations carried out to design the new GEPI spalling test are reported. Finally, the results of a validation test conducted with a small alumina bar are reported.

2 Theory

2.1 Propagation of an elastic wave in a thin rod

In a thin cylindrical rod, elastic stress waves propagate in a state of one-dimensional stress. Dynamic equilibrium of a thin slice of the bar allows a partial derivative equation to be written to describe the wave propagation:

$$\frac{\partial \sigma_x}{\partial x} = \rho \, \frac{\partial^2 u}{\partial t^2}. \tag{1}$$

In equation (1), ρ is the density and u is the displacement. Then, assuming a pure one-dimensional stress state, the axial stress σ_x in the linear elastic bar is given by Hooke's law and equation (1) can be rewritten as:

$$\frac{\partial}{\partial x} \, E \left(\frac{\partial u}{\partial x} \right) = \rho \, \frac{\partial^2 u}{\partial t^2}. \tag{2}$$

The propagation of a compressive or tensile elastic wave in a cylindrical bar is usually described by the second order hyperbolic partial derivative equation:

$$\frac{\partial^2 u}{\partial t^2} = C_0^2 \, \frac{\partial^2 u}{\partial x^2}. \tag{3}$$

Consequently, the celerity of elastic waves in a cylindrical rod C_0 is directly linked to the characteristics of the constitutive matter through the following relation:

$$C_0 = \sqrt{\frac{E}{\rho}}. \tag{4}$$

This simple approach provides a correct description of wave propagation as long as the wavelength of the loading pulse is significantly larger than the diameter of the elastic bar. If this condition is not fulfilled, the dispersive nature of the loading wave must be taken into account.

2.2 Dispersive effects in bars

Pochhammer in 1876 [13] and Chree in 1889 [14] independently derived the exact formulation for the wave propagation in an infinite cylindrical bar. Considering a sinusoidal wavetrain of angular frequency ω in an infinite cylindrical rod, the Pochhammer-Chree equations (Eqs. (5)–(9), [15]) allow the phase velocity C_p to be identified for a given wavelength. In equation (5), C_L and C_S correspond respectively to the longitudinal and shear wave speeds given by equations (8) and (9). In these

relations, the material density and the elastic parameters, i.e., Young's modulus E, the shear modulus G and Poisson's ratio ν are needed.

$$k^2 q \frac{J_0(qr)}{J_1(qr)} + \frac{1}{r}\left[-\frac{1}{2}\left(\frac{\omega}{C_S}\right)^2\right] + \frac{J_0(pr)}{J_1(pr)p}\left[\frac{1}{2}\left(\frac{\omega}{C_S}\right)^2 - k^2\right] = 0 \tag{5}$$

with

$$p = \sqrt{(\omega/C_L) - k^2}, \tag{6}$$

$$q = \sqrt{(\omega/C_S) - k^2}, \tag{7}$$

$$C_L = \sqrt{\frac{E\ (1-\nu)}{\rho\ (1+\nu)(1-2\nu)}}, \tag{8}$$

$$C_S = \sqrt{G/\rho}. \tag{9}$$

In the preceding relations, k corresponds to the wavenumber and J_0 and J_1 are the Bessel functions of the first kind. By studying equations (5)–(9), the multiple real roots can be identified numerically, each corresponding to a propagating mode. The first mode (largest root) provides the phase velocity C_P plotted in Figure 1 as a function of the bar radius-to-wavelength ratio: while the largest wavelengths are propagating at the wave speed C_0 defined in equation (4), high-frequency waves travel at a lower speed. For high values of r/λ, the phase velocity C_P tends asymptotically to the celerity of the Rayleigh surface wave.

3 Design of a 1D-stress spalling test

3.1 GEPI tests

The GEPI machine is a high pulsed power generator based on the strip line concept [9,10]. This machine allows ramp loadings spread over about 500 ns to be produced. This characteristic makes it a good candidate to perform quasi-isentropic experiments on inert materials [12]. Impact studies using high velocity flyer plates are another type of tests conducted with the GEPI machine [10].

Twenty-eight stages are connected in parallel. Considering a charging voltage of 80 kV, about 70 kJ is stored and released when the stages are simultaneously triggered. The current coming from the stages (up to 3.3 MA) flows to the center of the generator. It is concentrated in the load strip line, inducing an intense magnetic field in this area. The combination of high intensity current and strong magnetic field results in a pressure pulse being applied to the internal skin of the aluminum electrode (Fig. 2). The pressure P in the strip line is given by:

$$P(t) = k\ \frac{\mu_0}{2}\ \left(\frac{I(t)}{W}\right)^2, \tag{10}$$

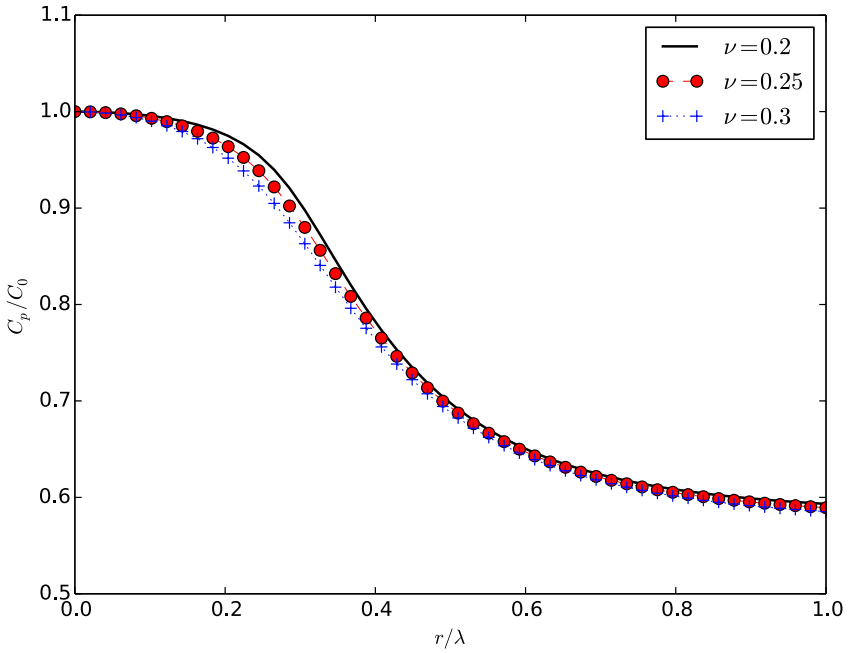

Fig. 1. Normalized phase celerity as a function of the radius-to-wavelength ratio for 3 values of Poisson's ratio.

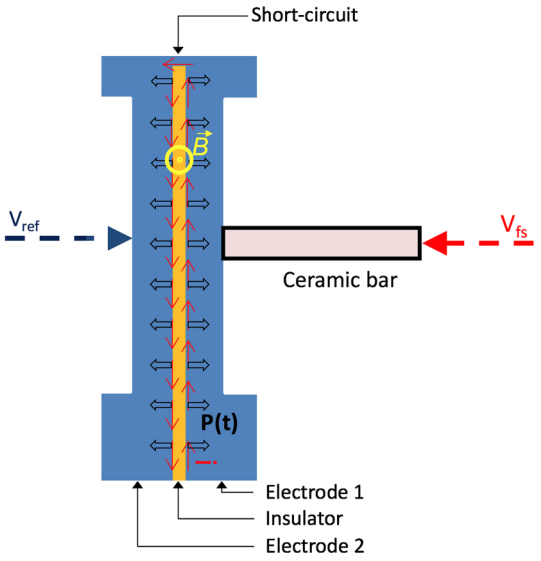

Fig. 2. GEPI configuration to conduct spalling test in a 1D-stress state.

where μ_0 corresponds to the free space magnetic permeability and $I(t)$ is the temporal evolution of the current in the strip line. Finally, W is the electrode width and k is a loss coefficient. The pressure range attainable with GEPI is linked to two main aspects: first, as illustrated by equation (10), increasing the electrode width W leads to apply a lower amplitude of the pressure pulse being applied on the internal skin of the load. Second, the possibility of disconnecting the stages one by one and adjusting

their charging voltage allows the intensity of the current to be mastered accurately, and thus the amplitude of the loading wave. However, the duration of the pulse generated by GEPI is imposed. It is linked to the experimental configuration and to the physical characteristics of its main components.

As presented in Figure 2, the ceramic bar is placed in contact with the electrode. Two velocity measurements are performed. The first measurement V_{ref} points out the free surface of the aluminum electrode. This reference signal is aimed at checking the dynamic pulse produced by the GEPI generator. The second laser is directed toward the free surface of the specimen (V_{fs} in Fig. 2). The velocity profile allows the dynamic tensile strength σ_{spall} of the ceramic sample to be computed using an acoustic approximation proposed by Novikov et al. [16], given by equation (11). In this relation, ΔV_{pb} is the pullback velocity, i.e., the difference between the maximum velocity and the value at the first rebound. The accuracy of this formula has been verified using numerical simulations for various damage kinetics [17].

$$\sigma_{spall} = \frac{1}{2}\ \rho\ C_0\ \Delta V_{pb}. \tag{11}$$

3.2 Numerical design of specimen geometry

The design of a spalling test conducted with the GEPI generator needs to take into account two contradictory aspects. First, the cylindrical specimen diameter has to be limited, in order to neglect dispersion: the loading wave has to be stable and the stress level has to be homogeneous in every section of the bar. On the other hand, the bar diameter has to be large enough to make the experimental procedure easier: ensuring good contact conditions between the face of the bar and electrode or pointing the laser beam toward the specimen free-end in order to measure the velocity profile are difficult operations when the sample has a very small diameter.

In order to study the wave propagation in an elastic ceramic bar, numerical simulations have been conducted with the commercial code Abaqus/explicit. The ceramic is considered as a linear elastic material. The main properties used in the simulation, gathered in Table 1, are representative of a dense alumina ceramic. Computations have been carried out for bars having diameters of 1, 3, 6 and 9 mm. In the simulations, the ceramic sample is long enough to be considered as semi-infinite (70 mm). An experimental pulse (G692, see [8]) is applied as a pressure load on the face located at $z = 0$ (Fig. 3). In every simulation reported in this work, the mesh is composed of 8-node reduced order linear hexahedral elements (C3D8R).

Preliminary numerical simulations have been carried out with the 6 mm diameter bar considering elements with different characteristic sizes. In Figure 5 are plotted the time evolution of the mean axial stress in two sections of the specimen ($z = 15$ mm and $z = 30$ mm). Each curve corresponds to the axial stress averaged over all the elements composing a given section of the bar. They are plotted for 3 different meshes. The reference mesh size L_e is equal to 0.1 mm (Fig. 4). This fine mesh size is chosen to accurately discretize the circular section of the ceramic sample and to capture the dispersion of the loading wave. For the second mesh with $L_e = 0.2$ mm, signals are very similar to the reference ones: considering peak values at $t \approx 2$ μs and $t \approx 4$ μs, differences with results obtained using the reference mesh are lower than 2%. When element size is increased to $L_e = 0.4$ mm, the pulse shape is slightly smoothed and shifted but signals are still consistent with reference curves. After 30 mm of propagation, the maximum compressive stress is 7% lower than reference mesh data. The smallest size of elements ($L_e = 0.1$ mm) has been used for every simulations reported thereafter.

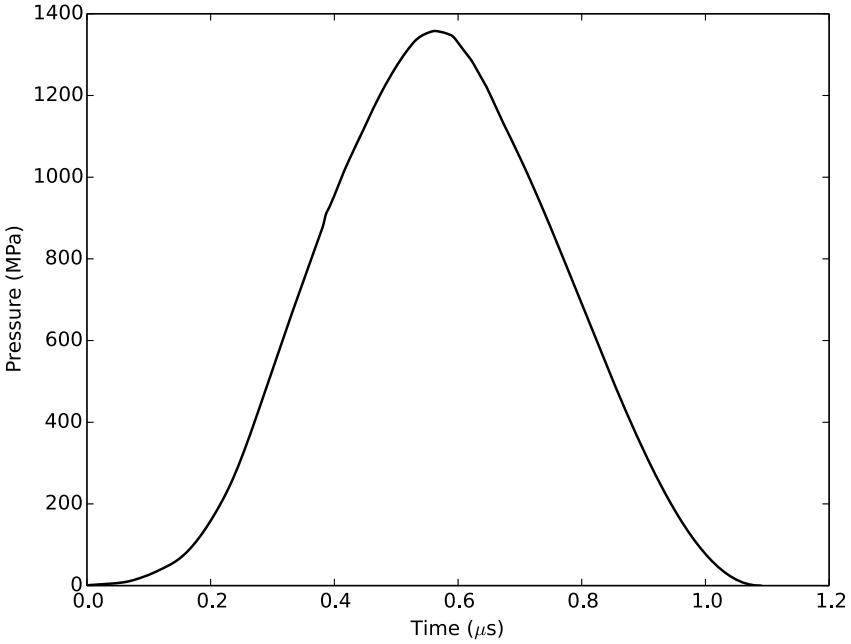

Fig. 3. Stress pulse $\sigma(t)$ applied to the specimen in the numerical simulations.

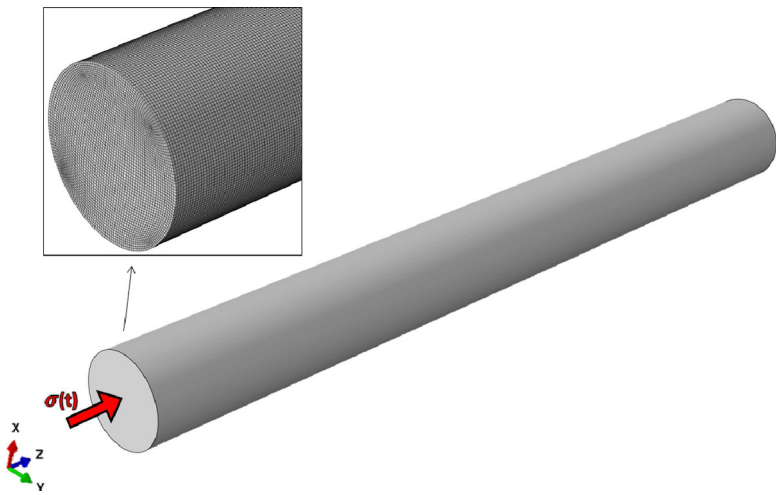

Fig. 4. 3D mesh of the ceramic bar used in the numerical simulations (specimen diameter: 6 mm, 2.03×10^6 elements, $L_e = 0.1$ mm).

Table 1. Ceramic properties used in the numerical simulations.

Density	3900 kg/m^3
Young modulus	370 GPa
Poisson ratio	0.24

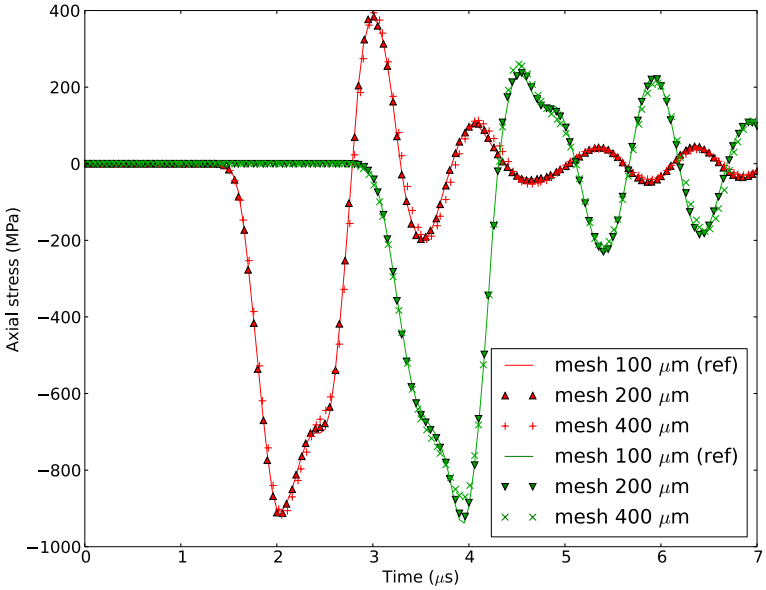

Fig. 5. Mesh size influence on the axial stress averaged over all the elements composing the section at $z = 15$ mm (red) and $z = 30$ mm (green) for a specimen diameter of 6 mm.

In Figure 6, the time evolution of the axial stress detected at $z = 15$ mm and $z = 30$ mm are presented. These results represent the minimum and maximum envelopes and the average of axial stress in all of the elements composing the section. Regarding these numerical results, the choice of a 3 mm diameter appears to be a good compromise: first, the shape of the elastic wave is stable between $z = 15$ mm and $z = 30$ mm, and a good homogeneity of the axial stress is obtained in a given section. Second, this dimension simplifies the experimental procedure: the specimen surface need to be glued, in order to ensure the contact quality between the electrode and ceramic sample. Moreover, the presetting of the laser interferometer used to measure the velocity directly on the free-surface of the specimen is very difficult for a very thin rod.

4 Experimental validation

The numerical simulations reported in the previous section demonstrate that the use of a 3 mm diameter alumina specimen allows the homogeneity of the stress field to be guaranteed during the pulse propagation. A spalling test was conducted with the GEPI generator on a small bar in the configuration presented in Figure 2. The diameter and length of the specimen are respectively 3 mm and 30 mm. In the validation test, the alumina bar is adhered to the aluminum electrode (electrode width is 52 mm and thickness is 2 mm). The pressure pulse being applied to the internal face of the electrode, computed with equation (10), is given Figure 7.

The velocity profiles measured on the free-surface of the electrode (reference signal) and on the free-surface of the alumina specimen are presented in Figure 8. Using equation (11), the dynamic strength of the ceramic can be calculated from the pull-back velocity ΔV_{pb}. In this test, the spalling strength of the alumina is 802 MPa for a strain-rate at failure roughly estimated to 2×10^4 s^{-1}. It should be noted

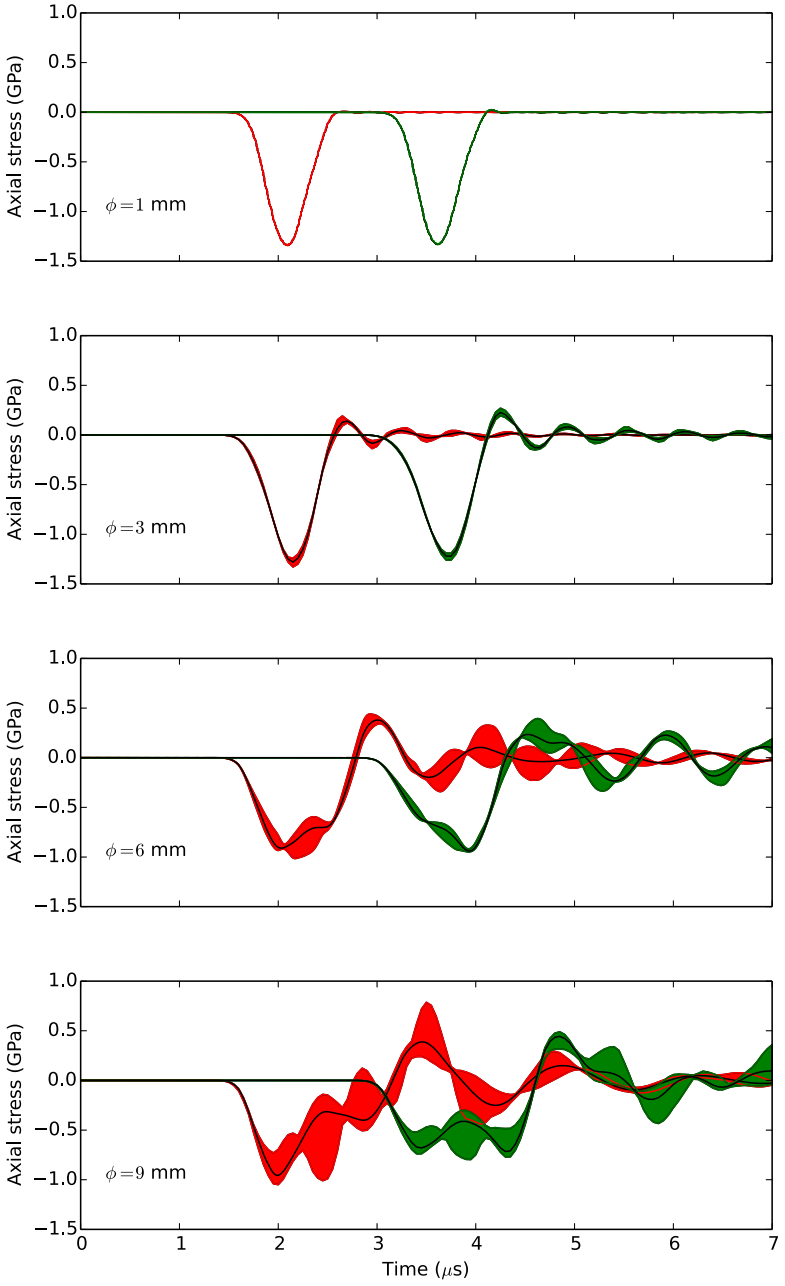

Fig. 6. Time evolution of the axial stress at $z = 15$ mm (min and max envelopes filled in red) and $z = 30$ mm (min and max envelopes filled in green) for 4 bar diameters ranging from 1 to 9 mm; the black lines are averages over all of the finite elements in the considered section.

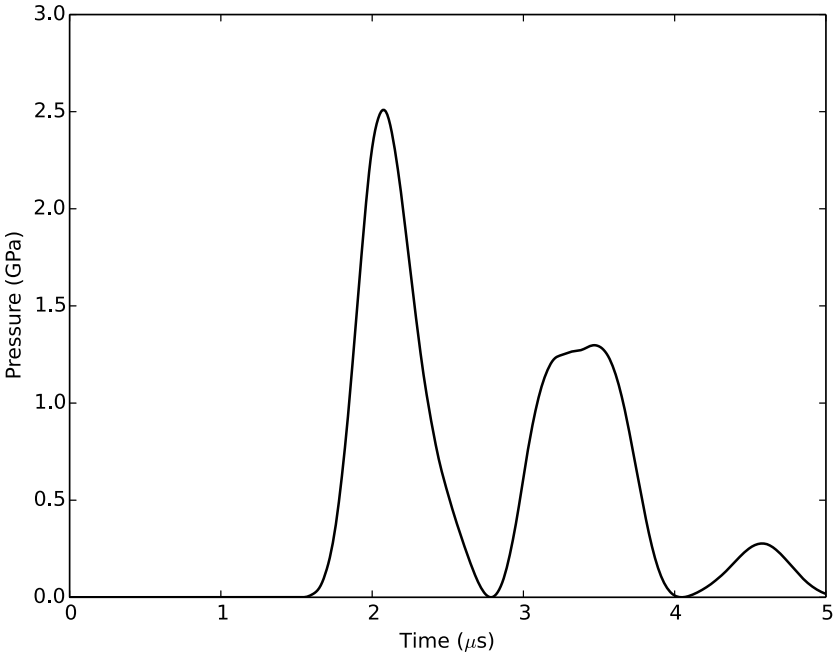

Fig. 7. Pressure pulse applied to the internal face of the aluminum electrode, computed from the time evolution of current (Eq. (10), $k = 0.975$) – test G1245.

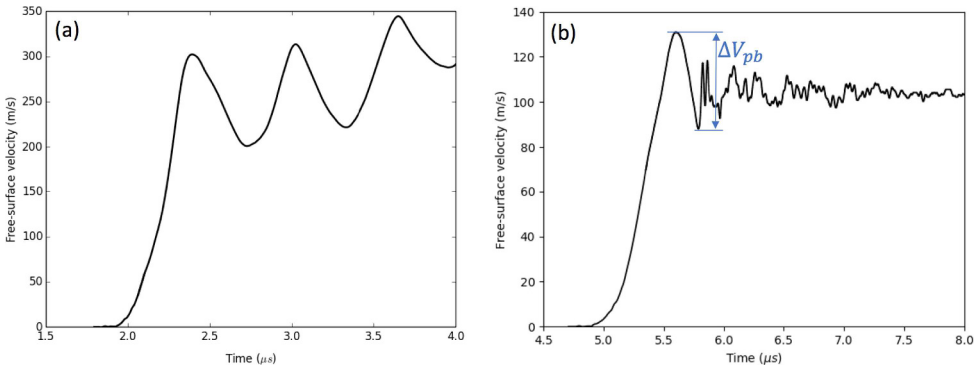

Fig. 8. Experimental free-surface velocity profiles measured (a) on the electrode (reference signal) and (b) on the ceramic cylindrical specimen – test G1245.

that this dynamic strength is high in comparison with the results obtained with another alumina in previous studies [7,8]. However, this experiment has been conducted in a 1D-stress state while previous spalling tests were done in a 1D-strain state.

5 Conclusions

The spalling strength of ceramics is usually determined by using plate impact experiments. Recently, the use of ramp loading produced by a high-pulsed power generator has offered interesting advantages to characterize brittle materials like ceramics.

In this work, a new experimental configuration is proposed to conduct spalling tests in a 1D-stress state at very high loading rates. The use of a high-pulsed power machine allowed a quasi-sinusoidal pressure pulse to be generated. This 1 μs duration pulse is transmitted to the tested sample, which is a thin ceramic rod. This cylindrical specimen has been designed thanks to finite element simulations to determine the best compromise between wave dispersion and experimental constraints. Finally, a validation test has been conducted on a cylindrical specimen made of alumina ceramic. In this test, a very high dynamic strength has been obtained (802 MPa).

Additional experimental efforts are needed to understand how the loading state influences the dynamic tensile strength of brittle materials like ceramics. To do so, two specimens of the same material (a small bar in a 1D-stress state and a plate specimen in a 1D-strain state) will be tested in a single spalling experiment with the GEPI generator.

This work was supported by the French General Directorate for Armament (DGA), of the Ministry of the Armed Forces. The author is also grateful to J.J. Royer (CEA-Gramat) for his technical contribution to this project.

References

1. F. Longy, Ph.D. thesis, Centre d'Etudes de Gramat, 1988
2. L.H.L. Louro et al., J. Phys. IV France **49**, C3-333 (1988)
3. A. Cosculluela, Ph.D. thesis, Centre d'Etudes de Gramat, 1992
4. N.H. Murray et al., J. Appl. Phys. **84**, 734 (1998)
5. F. Gálvez, J. Rodriguez, V. Sánchez, J. Phys. IV France **7**, 151 (1997)
6. S. Walley, Adv. Appl. Ceram. **109**, 446 (2010)
7. B. Erzar, E. Buzaud, Eur. Phys. J. Special Topics **206**, 71 (2012)
8. J.L. Zinszner et al., J. Mech. Phys. Solids **85**, 112 (2015)
9. G. Avrillaud et al., in *Proceedings of the 14th IEEE International Pulsed Power Conference* (2003), p. 913
10. P.L. Hereil, F. Lassalle, G. Avrillaud, Shock Compress. Condens. Matter Conf. **706**, 1209 (2004)
11. J.L. Zinszner et al., Philos. Trans. R. Soc. A **375**, 20160167 (2016)
12. B. Erzar, E. Buzaud, P.Y. Chanal, J. Appl. Phys. **114**, 244901 (2013)
13. L. Pochhammer, J. Reine Angew. Math. **81**, 324 (1876)
14. C. Chree, Trans. Cambr. Philos. Soc. **14**, 250 (1889)
15. M. Redwood, *Mechanical waveguides* (Pergamon Press, New York, 1960)
16. S.A. Novikov et al., Fiz. Metall. Metallovedeniye **4** (1966)
17. B. Erzar, P. Forquin, Exp. Mech. **50**, 941 (2010)